

A sequential selective dissolution method to quantify storage and stability of organic carbon associated with Al and Fe hydroxide phases



Katherine Heckman^{a,1}, Corey R. Lawrence^{b,*}, Jennifer W. Harden^c

^a USDA Forest Service, Northern Research Station, 410 MacInnes Drive, Houghton, MI 49931, United States

^b U.S. Geological Survey, Geosciences & Environmental Change Science Center, Denver Federal Center, MS 980, Box 25046, Denver, CO 80225, United States

^c U.S. Geological Survey, 345 Middlefield Road, Menlo Park, CA 94025-3561, United States

ARTICLE INFO

Editor: I. Kögel-Knabner

ABSTRACT

Stabilization of SOM (soil organic matter) is regulated in part by sorption and desorption reactions happening at mineral surfaces, as well as precipitation and dissolution of organo-metal complexes. Fe and Al hydroxides play a particularly significant role in SOM stabilization in soils due to their ubiquitous distribution and their highly reactive surface properties. Iron and Al hydroxides exist in soils across a wide spectrum of crystallinity, ranging from dissolved Fe and Al cations which combine with organics to form organo-metal precipitates to the more crystalline end members, goethite and gibbsite, which sorb SOM through a variety of molecular interactions. Though the importance of these sorption and precipitation reactions has long been recognized, the distribution of SOM among Fe and Al hydroxides of differing crystallinity has not been well quantified, nor has the timescale over which these stabilization mechanisms operate. In an attempt to measure the distribution of organic C among (i) Al- and Fe-humus complexes (ii) short-range-order (SRO) Al and Fe hydroxide surfaces and (iii) crystalline Fe oxyhydroxide surfaces, a single method combining several selective mineral dissolutions was applied to soils of four different genesis (a tropical forest Andisol, a temperate forest basaltic Mollisol, a Mediterranean coastal prairie Mollisol, and a northern mixed hardwood forest Spodosol). The traditional reactants used in selective dissolutions were replaced with carbon-free analogues so that the carbon released along with the Fe and Al at each stage of the selective dissolution process could be measured. Selective dissolutions were performed sequentially: Na-pyrophosphate (organo-Al and Fe complexes) followed by hydroxylamine (SRO Al and Fe hydroxides) followed by dithionite-HCl (crystalline Fe hydroxides). Carbon, Al, and Fe concentrations, as well as radiocarbon abundance were measured in the solutions yielded by each stage of the selective dissolution process. Results suggest that precipitation of organo-metal complexes (Na-pyrophosphate extractable C) often accounts for the largest pool of stabilized C among the three selectively dissolved pools, but these complexes were ¹⁴C enriched in comparison to C from the other selectively dissolved pools and the residual C left on crystalline mineral surfaces after all three stages of selective dissolution. Hydroxylamine and dithionite-HCl extractable C pools were, on average, small and often below detection level in temperate soils. However, radiocarbon values for these C pools were generally depleted in comparison to other pools. These results suggest variation in organo-mineral complex stability is associated with degree of crystallinity of the mineral phase. Overall, this work suggests that sequential selective dissolution methods are a promising tool for characterizing the content and isotopic composition of soil C associated with distinct organo-mineral and organo-metal associations.

1. Introduction

In the past decade, there has been an increasing interest in the influence of the reservoir of terrestrial carbon (C) on atmospheric CO₂ concentrations, particularly in the context of climate change and climate change mitigation (Lal et al., 2012). The rate at which soil organic

C (SOC) is degraded and returned to the atmosphere as CO₂ is determined in part by soil physiochemical C stabilization mechanisms such as occlusion of organics within aggregate structures, sorption of organics to mineral surfaces, and co-precipitation of organics with dissolved metals. The amount of SOC stabilized through various physiochemical interactions with soil mineral or metal phases varies widely

* Corresponding author.

E-mail addresses: kaheckman@fs.fed.us (K. Heckman), clawrence@usgs.gov (C.R. Lawrence), jharden@usgs.gov (J.W. Harden).

¹ Authors share first author status.

but typically accounts for the majority of C in soils (Kögel-Knabner et al., 2008 and references therein). In order to better assess the vulnerability of these large SOC stocks to climate and land use change, improved quantification of the relative abundance and strength of differing organo-mineral/metal stabilization mechanisms is required.

Organo-mineral reactions are known to increase the mean residence time (MRT) of SOC, as evidenced by radiocarbon-based modeling and comparison to SOC fractions unassociated with mineral phases (Trumbore, 2009). In most soils, however, mineral stabilized C is not a homogenous pool and is instead thought to be composed of sub-fractions with distinct and differing MRTs (Sollins et al., 2009; Hall and Silver, 2013). Yet the cause and extent of such variation has not been well quantified. Organics may be bonded to the mineral phases in a variety of ways including weak electrostatic interactions such as H-bonding or Van der Waals forces, or less reversible bonds including cation bridging, anion bridging, ligand exchange and pi-pi electron interactions (Essington, 2004; Keiluweit and Keber, 2009). Integration of these stabilization mechanisms and their influence of SOC turnover into soil models requires a repeatable and flexible approach for partitioning soil mineral fractions and the SOC associated with them.

Prior studies have leveraged differences in soil physical properties (e.g., texture and mineralogy) in order to explain variations in SOC turnover and composition. In general, the clay-sized fraction (< 0.22 µm in diameter) is considered to have the greatest influence on SOC abundance and turnover (Tiessen et al., 1984; Oades, 1988). Consequently, soil texture is often applied as a predictor of C turnover rates in soils (e.g., Han et al., 2014). Clay mineral composition has also been shown to influence the abundance of SOC, with 2:1 expanding phyllosilicate clays generally sorbing more C than non-expansible 1:1 phyllosilicates such as kaolinite (von Lützwow et al., 2006; Saidy et al., 2012), and with C sorption potential increasing with the amount of structural charge induced by isomorphic substitution (Kahle et al., 2002, 2003). Although texture is often a reasonable predictor of SOC storage and turnover, an increasing number of studies have indicated that Al and Fe oxyhydroxide phases may have an even greater influence on SOC (e.g., Torn et al., 1997; Percival et al., 1999; Eusterheus et al., 2005; Rasmussen et al., 2006;). Aluminum and iron are the third and fourth most abundant elements in soil, respectively, and their various oxyhydroxide phases are largely ubiquitous across climates and ecosystems (Cornell and Schwertmann, 2003), though abundances vary widely. Iron- and Al-oxyhydroxide phases exist across a continuum of crystallinity and reactivity, with the relative distribution of minerals within the spectrum determined by soil age, climate, and parent material, among other factors. These oxyhydroxide phases can be inherited from parent material, but are often precipitated from soil solution as primary minerals undergo weathering and dissolution. Poorly crystalline, or short-range order (SRO), hydroxide phases often form at intermediate stages of soil development, where weathering conditions result in high concentrations of dissolved Si and Fe or Al (Parfitt, 2009). With increasing weathering, however, SRO minerals typically mature to more crystalline phases through Ostwald ripening, a process whereby particles of smaller radius and higher solubility are deposited onto larger more crystalline particles (Tadros, 2013). Furthermore, the formation and persistence of aqueous phase organo-metal complexes complicates the trajectory of mineral development and, depending on conditions, may inhibit or serve as a precursor to the formation of SRO or other Al and Fe oxyhydroxide minerals (e.g., Lawrence et al., 2014).

There have been a variety of studies aimed at addressing the importance of various Fe and Al oxyhydroxide mineral phases. However, these studies often focus on only one or two mineral phases and typically do not consider the dynamic nature of soil organo-mineral/metal reactions in time or space. SRO mineral phases have been shown to influence SOC abundances (Torn et al., 1997; Masiello et al., 2004; Rasmussen et al., 2005) particularly in volcanic soils, where SRO minerals are formed from extrusive igneous parent materials during intermediate stages of weathering. These high specific surface area

minerals with an abundance of reactive hydroxyl groups can cover other mineral and organic surfaces and may dominate surface chemistry characteristics soils where they form (Kögel-Knabner et al., 2008). A greater role of crystalline Fe hydroxide phases in soil C cycling has also been proposed based on significant correlations between estimates of crystalline Fe abundance and mineral-associated SOC abundance (Mikutta et al., 2006). Amorphous Fe and organo-Al complexes (e.g., the complexation of organic compounds with dissolved Al and Fe) may additionally account for a significant fraction of the mineral-bound C pool (Wagai and Mayer, 2007; Wagai et al., 2013; Lawrence et al., 2015) though their stability and MRT in comparison to organics stabilized through surface complexation reactions is not well understood.

In order to facilitate more widespread comparisons of the various classes of organo-mineral/metal protection of SOC, a consistent methodology needs to be applied, which can distinguish between SOC stabilized through various processes. Selective mineral dissolutions have been widely used to estimate the proportion of various mineral classes including organo-metal complexes, SRO, oxyhydroxides, and crystalline clays. However, these varied methods are inconsistently applied and rarely combined in a systematic fashion. By combining and applying such methods sequentially, it should be possible to determine relative abundances of each mineral class and to compare these results across a variety of soil types. There are, however, some problems with the application of these methods to quantification of mineral-associated SOC. First, there is evidence that such methods are not as selective as our interpretations would suggest (Pansu and Gautheyrou, 2006), with overlap or inconsistencies in our interpretation of various mineral phases dissolved (Kaiser and Zech, 1996). Second, the reagents used for many of the traditional methods contain organic compounds (e.g. oxalate, citrate) and are thus not appropriate for measuring the SOC liberated during mineral dissolution. Despite these limitations, selective dissolution offers an appealing approach because it is more selective than physical methods of clay mineral separations. As such, variations of traditional protocols have been developed using inorganic reagents, to allow for measurement of SOC associated with each selectively dissolved mineral fraction.

The goals of this work are to evaluate the utility of sequential selective dissolution methods for characterizing turnover of different mineral-bound SOC pools and to improve our understanding of heterogeneity in mineral protection on SOC turnover across different soil types by testing the following hypotheses:

1. A sequential selective chemical dissolution technique allows for quantification of soil mineral functional classes and measurement of the SOC associated with them.
2. The abundance of secondary Fe and Al mineral phases, and by association the abundance of SOC, vary across different soil types.
3. The radiocarbon content, and by implication the mean residence time, of SOC will vary depending on the abundance and type of secondary mineral phases.

To test these hypotheses, we have developed and applied a sequential selective mineral- dissolution methodology to four different soil/ecosystem types: a Spodosol, a forested Mollisol, a grassland Mollisol, and an Andisol. We used a variety of analyses, including radiocarbon, to evaluate both the aqueous extraction products and the residual soil solids, in order to determine the relative abundance of SOC associated with each mineral class and to determine if those pools were dominated by SOC with distinct radiocarbon signatures.

2. Methods

2.1. Soil sampling

We have compared the composition of soil mineral functional classes across four distinct soil/ecosystem types, the site and soil

characteristics are given in Tables 1 and 2. The Spodosol samples are from the U.S. Geological Survey (USGS) soil archive in Menlo Park, CA, and were collected in 1992 from northern Michigan, USA (Schaetzl, 2002). This soil developed on arkosic intertidal sand and had a well-developed spodic horizon; only the A, E, and two Bhs horizons were assessed in this study. The forested Mollisol was sampled in 2008 near Flagstaff, Arizona, USA (Heckman et al., 2011). The soil developed from basaltic bedrock with substantial dust inputs, and is very Fe and clay rich with a well-developed argillic horizon. Density separation data from this soil were previously reported in Heckman et al. (2014). The grassland Mollisol developed on marine terraces comprising Miocene Santa Cruz Mudstone and well-sorted and poorly cemented Santa Margarita Sandstone near Santa Cruz, California, USA (White et al., 2008). Chemical weathering of these paleo-marine sediments resulted in extensive formation of secondary kaolinite clay and redox/rhizosphere processes, which drive significant mottling and the formation of Fe-oxide nodules (White et al., 2008; White et al., 2009; Schulz et al., 2010). Samples from this site were collected in 2012 from a 125 kyr terrace. The Andisol pedon, developed from weathered tephra, was sampled in 2012 from the Hawaii Experimental Tropical Forest on Hawaii Island, Hawaii, USA. The pedon included in the current study was taken from the ‘WPL 1204’ sample site described in Litton et al. (2011). The Andisol was rich in Fe and Al, with an abundance of poorly crystalline phases. All soil samples were air-dried and sieved at 2 mm prior to processing and analyses. The soils examined here did not contain appreciable amounts of carbonates, so no pretreatment to remove inorganic carbon was performed; the results are described below. Due to the differences in year of sampling among the soils, there is variance in the soil radiocarbon values associated with incorporation of radiocarbon from above-ground nuclear arms testing (often referred to as “bomb C”). A comparison of atmospheric radiocarbon values at the times of sampling is given in Supplementary Fig. 1.

2.2. Density separation

We density separated soils using a sodium-polytungstate solution (SPT) following methods adapted from Strickland and Sollins (1987) and Swanston et al. (2005). Despite differences in the soils types studied here, we applied a consistent density threshold of 1.65 g cm^{-3} to all samples in order to facilitate comparisons of a standard methodology across the various soils and depths. Briefly, we mixed 20 g of soil with 75 ml of SPT in a 175 ml conical bottomed Nalgene centrifuge tube and stirred gently for 30 s. We then let samples rest on the bench-top for 45 min before centrifuging them at 2800 RCF for 1 h. Following centrifugation, we aspirated the supernatant, including all particles floating at a density of 1.65 g cm^{-3} , into a side-arm flask, then transferred it to vacuum filtration apparatus and washed it with 600 ml of deionized water over a $0.8 \mu\text{m}$ polycarbonate filter. We then dried the filters at 90°C . We refer to the organics isolated through flotation, which are assumed to not be stabilized through association with the mineral matrix, as the ‘free-light fraction.’ Next we added an additional 50 ml of SPT solution to the centrifuge tubes, and mixed the remaining sample with a bench-top mixer (Polymix PX-SR 90 D, Kinematica Inc.,

Bohemia, NY) for 1 min at 75% of maximum speed. We then sonicated the samples at maximum power for 3 min and 70% pulse with a Branson digital sonifier fitted with a 102C (CE) model microtip (Branson Ultrasonics Corporation, Danbury, CT). After sonication, we left the samples to sit overnight to allow proper separation of organic and mineral particles. The following day, we centrifuged, aspirated, washed, and dried the collected organic fraction as described above. We assumed the organic material isolated in this step of the procedure was sourced from within aggregate structures, and we refer to it as the ‘occluded fraction.’ We then washed the remaining soil pellet from the centrifuge tubes, the ‘mineral fraction,’ with 600 ml of deionized water through repeated dispersion, centrifugation and aspiration of the supernatant. Following this washing procedure, we dried the remaining mineral fraction at 90°C . Finally, we ground each density separate in order to homogenize the samples prior to further analyses.

2.3. Selective dissolution extractions

Starting with the mineral fraction from the density separation procedure, we selectively dissolved Al and Fe phases of varying crystallinity and their associated organic matter using three previously published chemical extraction methods (Dahlgren, 1994; Parfitt and Childs, 1988; Wagai and Mayer, 2007). We applied these methods in sequential manner in order to quantify the amount of total soil C and the associated Fe and Al content of the selectively dissolved mineral phases, without the possibility of overlap. We first extracted the mineral fractions with sodium pyrophosphate (Na-pyrophosphate), which is assumed to target organo-metal complexes. Next, we extracted the residual from the first stem with hydroxylamine, which is a carbon-free alternative to acid ammonium oxalate extractions that targets SRO and other non-crystalline phases (Ross et al., 1985). Finally, we used a modified dithionite (Wagai and Mayer, 2007) extraction to dissolve any remaining crystalline Fe and Al phases.

We performed two different batches of extractions. In the “solution-phase” batch of measurements, C concentration, radiocarbon measurements, and extracted metals (Al and Fe) were made directly on the supernatant solution after reaction with the soil sample. In the “solid-phase” batch of measurements, C concentration and radiocarbon measurements were made on the soil material directly after each stage of extraction. We then calculated the amount of SOC extracted as the difference in C mass before and after each step of the extraction procedure. We measured metal concentrations only for the solution-phase approach. The solid-phase approach was applied following several complications posed by performing radiocarbon measurements on the liquid samples from the solution-phase approach (presented in discussion) and required starting with greater sample mass in order to collect subsamples for analyses and tracking of sample masses throughout the sequential extraction. Data from both batches of extractions are presented, with the solution-based data used to validate the solid-based approach. For each batch of extractions, we applied the three extraction methods sequentially. We conducted the solution-phase extraction in triplicate. Replicate extractions were measured individually for C and metal concentrations but because of the high cost of analysis and to

Table 1
Site characteristics for the soils examined.

Soil	MAT	MAP	Ecosystem Type	Landform	Soil Age	Parent material	Taxonomic Classification
Spodosol	8 °C	810 mm	Mixed coniferous-deciduous hardwood forest	Valley floor	10 ka	arkosic intertidal sand	Sandy, mixed, frigid Entic Haplorthod
Forested Mollisol	9 °C	675 mm	Temperate ponderosa pine forest	Backslope	10 ka	basalt	Clayey-skeletal, mixed, superactive, mesic Typic Plaeustoll
Grassland Mollisol	11 °C	500 mm	Oak grassland	Marine terrace	65 ka	arkosic sand/sandstone	Loamy, mixed, mesic, superactive Typic Haploxeralf
Andisol	16 °C	3180 mm	Tropical montane Wet forest	Backslope	20 ka	weathered tephra	Hydrous, ferrihydritic, isothermic Acrudoxic Hydruand

Table 2
Soil physiochemical characteristics.

Soil	Year Sampled	Depth (cm)	Horizon	Texture	Mineralogy	Bulk % C
Spodosol Kalkaska series	1992	5–8	A	Sand	Q, F, H, Go	5.30
		22–36	E	Sand	Q, F, H, Go	2.60
		36–56	Bhs	Sand	Q, F, H, SRO, Go	1.70
		56–76	Bhs	Sand	Q, F, H, SRO, Go	1.50
Forested Mollisol	2008	0–10	A	Loam	Q, F, M, Ka, Sm, Vr, Il, SRO, Go, Ma	4.90
		10–27	Bt1	Clay	Q, F, M, Ka, Sm, Il, SRO, Go, Ma	1.30
		27–42	Bt2	Clay	Q, F, M, Ka, Sm, Vr, Il, SRO, Go, Ma	1.00
		42–75	Bt3	Clay	Q, F, M, Ka, Sm, Vr, Il, SRO, Go, Ma	0.70
Grassland Mollisol	2012	0–15	A	Silty loam	Q, F, Ka, Sm, SRO, Go	2.40
		16–30	A	Silty loam	Q, F, Ka, Sm, SRO, Go	1.80
		31–42	A	Silty loam	Q, F, Ka, Sm, SRO, Go	0.90
		43–60	AB	silty loam	Q, F, Ka, Sm, SRO, Go	0.50
Andisol ^a Honokaa series	2012	0–10	OA	Silty clay loam	M, Ka, A, SRO, G, Go, Ma	27.20
		10–30	Bw1	Silty clay loam	M, Ka, A, SRO, G, Go	11.00
		30–50	Bw2	Silty clay loam	M, Ka, A, SRO, G, Go, Ma	11.50
		50–88	Bw3	Silty clay loam	A, SRO, G, Go, Ma	9.20

Citation for data taken from soil survey: Soil Survey Staff, Natural Resources Conservation Service, United States Department of Agriculture. Official Soil Series Descriptions. Available online. Accessed [3/26/2014].

Q = quartz, F = feldspar, H = hornblende, M = mica, Ka = kaolinite, Sm = smectite, Vr = vermiculite, Il = illite, A = anatase, G = gibbsite, Go = Goethite, Ma = Magnetite, SRO = short-range order Fe & Al.

^a Horizon & mineralogy estimated from soil series description.

ensure sufficient C mass for measurement, we pooled the replicates for radiocarbon analysis. Because of limitations on how much solid we could extract, while ensuring a consistent solid to solution ratio we conducted the solid-phase extractions in duplicate but pooled the replicate samples prior to measurement of C concentration and isotope composition. In addition to unknown samples, we processed two types of control samples following identical protocols. The “reagent controls” consisted of clean sample tubes with no sample added, and the “sand controls” consisted of pre-baked (500 °C for 8 h) quartz sand in place of soil separates.

Details of the extraction procedure are as follows: First, we added approximately 1 g of each soil sample to a clean (pre-weighed) centrifuge tube and recorded the actual mass. Next, we added 40 ml of 0.1 M Na-pyrophosphate to each tube using a calibrated repipetter. Then we capped the tubes and vortexed them for 20 s before transferring them to a shaker table, where we shook them overnight in an end-to-end orientation. After shaking, we centrifuged each sample for 20 min at 20,000 RCF. Following centrifugation, we carefully decanted the supernatant into a 60 ml syringe and filtered the solution through a GD/X (Merck Millipore, Billerica, MA) syringe-tip filter into a 50 ml sample tube. In order to limit sample mass loss in the filter cartridge, we then pulled 5 ml of ultrapure H₂O through the filter in the reverse direction, back into the syringe. We added the fluid from this back-flush step back to the residual soil in the original centrifuge tube, containing the residual soil pellet. We then dried the residual pellets overnight at 60 °C or until all reagent/rinse H₂O had evaporated. Finally, we recorded the final dry-weight of the residual sample. Before the next extraction step, we used a clean glass rod to breakup and homogenize the dried sample pellets and then subsampled 0.2 g of this material from each replicate and pooled them prior to C analyses.

Following the first extraction step described above, we subjected the residual samples to the second (hydroxylamine) and third (dithionite-HCl) sequential extractions, which we conducted in a similar fashion following a similar sequence of steps including shaking, centrifugation, filtration, drying and subsampling. However, we reduced the volume of extractant in each successive extraction step, corresponding to the reduction in total solid phase sample mass (i.e., from mineral dissolution and from subsampling). For the second extraction, we added 40 ml of 0.1 M hydroxylamine prepared in a 0.25 N HCL solution to each centrifuge tube containing residual soil or control samples. For the third extraction, we added 30 ml of 0.5 M sodium dithionite to each sample. After addition of extractant solutions, we vortexed the samples for 20 s,

shook them overnight, centrifuged and then filtered them as described previously. For the last extraction, however, we did not immediately perform the filter back-flush procedure. Instead, we added 10 ml of 0.05 N HCl to the centrifuge tube and the residual soils were shaken for an additional 1 h. Next, we centrifuged the samples for a second time and filtered the HCl rinse (using the same filter from the previous step) into the sample tube already containing the 30 ml of dithionite extract. Then we back-flushed the filters with 5 ml ultrapure H₂O into the sample tube already containing the combined dithionite and HCl extracts (hereafter referred to as dithionite-HCl. After collection of each extraction, we dried the samples overnight, homogenized and weighed them prior to subsampling and compositing.

Fractions isolated and their assumed compositions are given in Supp. Table 1.

2.4. Soil carbon characterization

We analyzed the solution-phase samples for dissolved Al, Fe and Si on a Perkin Elmer Elan 6000 (PerkinElmer, Inc., Waltham, MA, USA using an inductively coupled plasma mass spectrometer (ICP-MS) at the USGS laboratory in Menlo Park, CA. Because of high Na concentrations in extracts, we typically needed to dilute samples by a factor of 25 to 50. We analyzed splits of the density separates and the residual material (i.e., solid-phase samples) collected post-extraction for total C content by combustion elemental analysis. In the case of this study, total C content is equivalent to soil organic C (SOC). Prior to measurement, using a mortar and pestle, we hand-ground the solid samples to pass an 80-mesh sieve. We then measured the C and N concentrations with a Carlo Erba elemental analyzer (Costech, Valencia, CA) at the USGS laboratories in Menlo Park, CA. Bulk density estimates for the soil examined in this study were not available, so we report the measured SOC in units of mg C g⁻¹ bulk-soil. We performed the radiocarbon analyses at the Center for Accelerator Mass Spectrometry (CAMS) of the Lawrence Livermore National Lab, and the University of California KECK Carbon Cycle Accelerator Mass Spectrometry Lab. We graphitized subsamples of solid-phase residuals and solution-phase extracts (when possible) through reduction of CO₂ in the presence of H₂ gas and an iron catalyst (Vogel et al., 1987). We then measured the radiocarbon abundance of each graphitized sample by accelerator mass spectrometry. Following standard protocol, we report sample measurements normalized to the absolute activity of the international radiocarbon standard, Oxalic Acid I (Stuiver and Polach, 1977).

2.5. Calculations

In the solid-phase approach, the C content of the extracted phase was calculated by simple difference in solid C content before and after the extraction. For example, the amount of C extracted by the Na-pyrophosphate was calculated by subtracting the C concentration of the post-pyrophosphate solid fraction from the C concentration of the pre-extraction, mineral fraction. These values are given in Supplementary Table 2c and d. In the case of calculated negative values, the value for the C extracted was set to zero.

Radiocarbon values for the extracted solutions were calculated based on the C distribution and radiocarbon values of the solid phases pre- and post-extraction.

$$Fm_{sol} = (Fm_{pre} - (fc_{post} \times Fm_{post})) / (1 - fc_{post}) \quad (1)$$

$$fc_{post} = C_{pre} / C_{post} \quad (2)$$

where Fm_{sol} is the Fraction modern value calculated for the respective extracted solution (i.e. Na-pyrophosphate, hydroxylamine, or dithionite); Fm_{pre} is the Fraction modern value directly measured on the solid sample prior to extraction of the solution of calculation; Fm_{post} is the Fraction modern value directly measured on the solid sample after extraction of the solution of calculation (i.e. if we are calculating the Fm value of the Na-pyrophosphate solution, Fm_{pre} would be the Fraction modern value measured on the mineral fraction, and Fm_{post} would be the Fraction modern value measured on the solid sample after extraction with Na-pyrophosphate); fc_{post} is the fraction of C remaining in the solid sample post-extraction relative to the amount of C that was in the solid sample prior to extraction, and C_{pre} and C_{post} refer to C contents expressed in values of mg C g^{-1} .

3. Results

3.1. Carbon content

The total concentrations of C in each soil type varied widely (Supp. Table 2). The Andisol exhibited an order of magnitude greater C concentrations, with nearly 300 mg C g^{-1} near the surface, declining to approximately 92 mg C g^{-1} below that. The forested and grassland Mollisol soils exhibited moderate values of 49 and 24 mg C g^{-1} at shallow depths, respectively. Both these profiles also exhibited similar decreases with depth, with minimum values $< 10 \text{ mg C g}^{-1}$ in the deepest samples. The Spodosol exhibited a moderate bulk C concentration (20 mg C g^{-1} between 5 and 8 cm) but declined to $\sim 3 \text{ mg C g}^{-1}$ in the eluvial E horizon (22–36 cm), then exhibited characteristic C enrichment ($\sim 10 \text{ mg C g}^{-1}$) in illuvial Bhs horizons at 36–76 cm.

The fraction of total sample mass recovered during the density separation was typically between 0.98 and 1.02 (data not shown), whereas the fraction of C recovered ranged from 0.7 at intermediate depths in both Mollisol soils to 1.8 in the eluvial horizon of the Spodosol (Supp. Table 2). Slightly more than half of the samples yielded C recovery values within 10% of the total bulk content. We did not account for C mobilized in the SPT solution, which more than likely accounts for the small C losses observed in several of the samples analyzed. One sample, the Spodosol from 5 to 8 cm, exhibited C loss of 70%, indicating significant losses during the density separation process. Only 20% of samples exhibit an excess of C based on the density separation measurements. These discrepancies are likely based on measurement errors in weighing and analyzing small and/or low C samples. This is particularly true for the eluvial horizon of the Spodosol where total C content was very low.

In all soils except the grassland Mollisol, the free-light fraction was typically most abundant at shallow depths ($> 20 \text{ cm}$) and declined rapidly with increasing depth (Fig. 1). Despite similarities in total C

content between the two Mollisol soils, they differed in the partitioning of C between density fractions (described below). The grassland Mollisol was dominated by mineral stabilized SOC at all depths, whereas the forested Mollisol profile exhibited an equitable distribution between free-light, occluded and mineral SOC. Occluded C accounted for a small fraction (0 to 4%) of total SOC in all soils except for the forested Mollisol, where it accounted for a depth-weighted average of 18%. Integrated across all depths, mineral stabilized C was the dominant SOC fraction accounting for approximately 56, 75, 90 and 93% in the forested Mollisol, Spodosol, Andisol and grassland Mollisol, respectively.

Results from the solution-phase method and the solid-phase methods were in general agreement (Fig. 2), though the Na-pyrophosphate extractable pool showed some variance between the two rounds of extractions in the grassland Mollisol and the Andisol. Additionally, the concentration of dissolved C extracted from the temperate soils using the solution-phase approach was small in comparison to the ionic concentration of the reagent, leading to a strong matrix effect and a low signal to noise ratio that negatively impacted detection limit and reproducibility of solution based C measurements for those samples.

The results of the sequential chemical dissolutions suggest that organo-metal complexes (extracted with Na-pyrophosphate) account for the majority of mineral-stabilized SOC in all but the forested-Mollisol soil, where residual SOC was the largest fraction (Fig. 2). Using the solid-phase method, SOC extracted with Na-pyrophosphate accounted for 16, 75, 64 and 63% of the total mineral SOC when averaged over all depths in the forested Mollisol, Spodosol, Andisol and grassland Mollisol, respectively. In the grassland-Mollisol and the Andisol soils, Na-pyrophosphate-extractable mineral SOC declined with depth. In the Spodosol, Na-pyrophosphate extractable SOC declined with depth to around 40 cm, where it then increased. Thus, the accumulation of C in the Bhs horizons appears to be primarily driven by formation of organo-metal complexes. Hydroxylamine-extractable SOC was most prevalent in the Andisol, where it was a relatively constant fraction of total mineral SOC with depth. Small amounts of hydroxylamine-extractable SOC were detectable in the Spodosol and forested Mollisol but none was measured in the grassland Mollisol. Significant amounts of dithionite-HCl extractable SOC was only measured in the Mollisol samples where it accounted for 16 and 26% in the grassland and forested Mollisol, respectively (based on solid-phase results). Residual SOC following extraction with all three dissolution reagents was present in all four soils, though relative amounts varied among soils and with depth. Measurement of C concentrations in replicate extractions indicated increasing error with each sequential step, with standard error of the extractions averaging 7, 15, and 35% of the mean values for the Na-pyrophosphate, hydroxylamine, and dithionite-HCl steps, respectively.

3.2. Radiocarbon enrichment and depletion of fractions

Density separations: In all soils, the mineral fraction was ^{14}C depleted (older) in comparison to the free-light fraction. Radiocarbon abundance (expressed as Fm) of the mineral fraction decreased with depth but the free-light fraction was comparatively stable with depth. In the forest Mollisol the occluded fraction was consistently the most ^{14}C depleted (Fig. 1), likely due to the presence of pyrogenic C in the occluded fraction. In the other soils, the occluded fraction was generally ^{14}C depleted in comparison to the free-light fraction (Supp. Table 3). The Andisol soil stored the greatest total amount of SOC and also the most ^{14}C -depleted SOC. Radiocarbon laboratory sample codes are given in Supp. Table 4 for data archiving purposes.

The presence of large amounts of P, N and S introduced to the extracts from the reagents (respectively) provided several obstacles to performing radiocarbon analysis. When combusted under vacuum in the first step of graphitization, the sample matrices produced large amounts of gas, which would cause the sample ampoules to explode. Measurements of Na-pyrophosphate extractions were generally

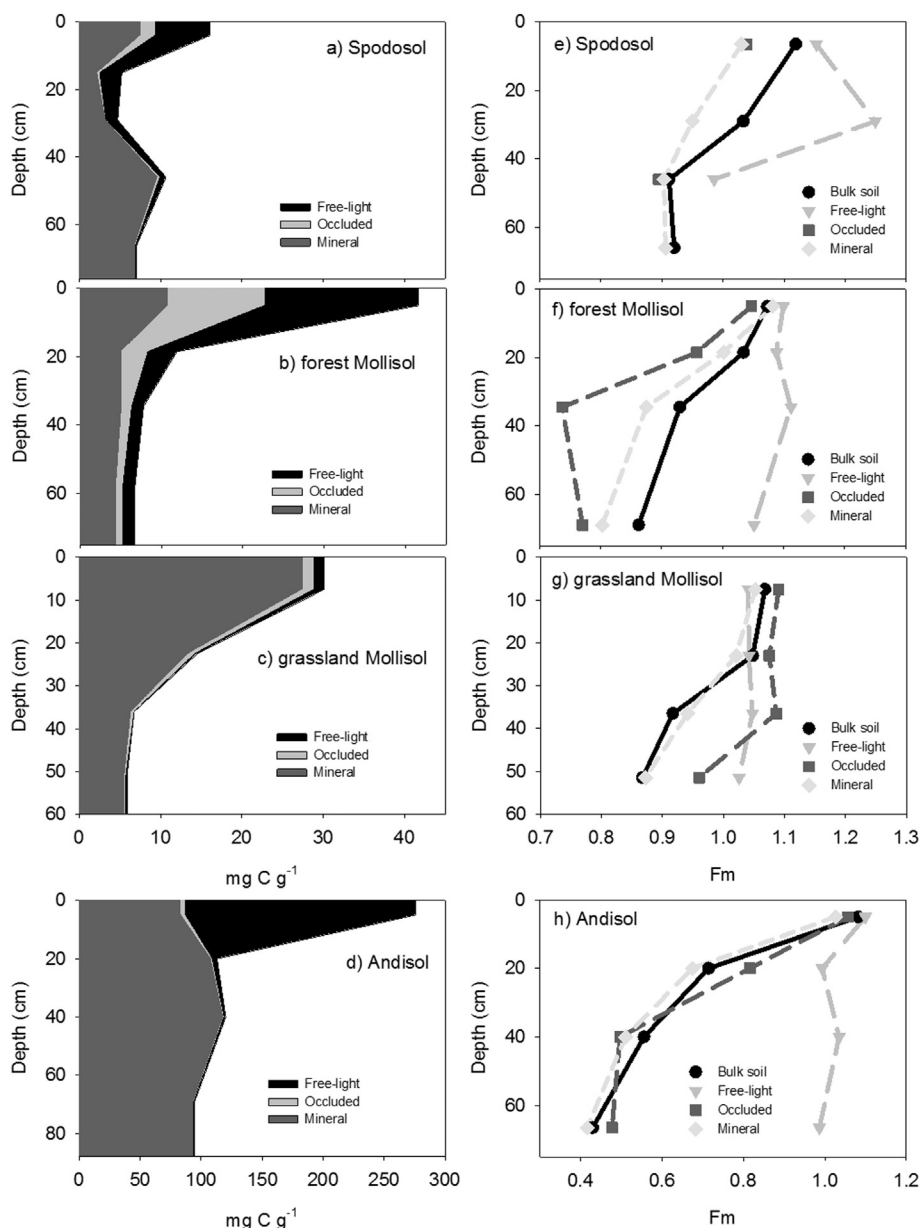


Fig. 1. a–d) Carbon distribution among density fractions. e–h) Fraction Modern (Fm) radiocarbon values for density fractions.

successful but the formation of N₂ gas from hydroxylamine added to the instability of those samples during combustion. Direct measurement of hydroxylamine extractions was abandoned after numerous failed attempts. High-purity dithionite reagent could not be located, so the dithionite used in the extractions contained ~0.1% C by weight, with a radiocarbon value of Fm ~0.14 ($\Delta^{14}\text{C} = 865\text{‰}$). This amount of C was enough to strongly influence the radiocarbon values measured on the extracted solutions from the temperate soils. Sulfur contained in the dithionite-HCl extracts often interfered with the graphitization process by poisoning the iron surfaces intended to catalyze the graphitization process, leading to incomplete or failed graphitization. Due to these complications, a second measurement approach was employed where C and radiocarbon measurements were made on the solid soil samples following each round of extraction instead of measuring the extractions directly. The C and radiocarbon concentrations of the extractions were then calculated by difference.

Carbon concentrations and radiocarbon signatures of Na-pyrophosphate extractable C varied significantly with depth and among soils (Figs. 2 and 3). Compared with the other extractants, the radiocarbon content of Na-pyrophosphate extracted C was generally similar to bulk

soil values but, where different, it could be ¹⁴C enriched or ¹⁴C depleted. In comparison with the mineral fraction and extraction residuals, Na-pyrophosphate extractable radiocarbon was almost always enriched (Fig. 3). In all soils except the Andisol, concentrations of SOC extracted with hydroxylamine and dithionite-HCl extracts were too low for their ¹⁴C abundance to be measured or calculated with any degree of confidence. Soil organic C concentrations extracted from the Andisol with hydroxylamine and dithionite-HCl fractions were an order of magnitude higher than those extracted from the other soils. As a result, we were able to estimate the ¹⁴C abundances of SOC extracted through direct measurement (solution-phase) or by the difference between pre- and post-extraction solid-phase measurements. In the subsurface horizons, SOC associated with extracts was not significantly different from the bulk soil, mineral fraction or residual SOC. Solution-phase measurements of ¹⁴C abundance in the OA horizon suggest that hydroxylamine and dithionite-HCl SOC fractions may be depleted in comparison to other fractions, but due to sample limitations solid-based calculations of ¹⁴C abundance were not possible. The residual SOC fraction retained in the soils after the sequential extraction procedure was the most ¹⁴C-depleted fraction in the other three soils.

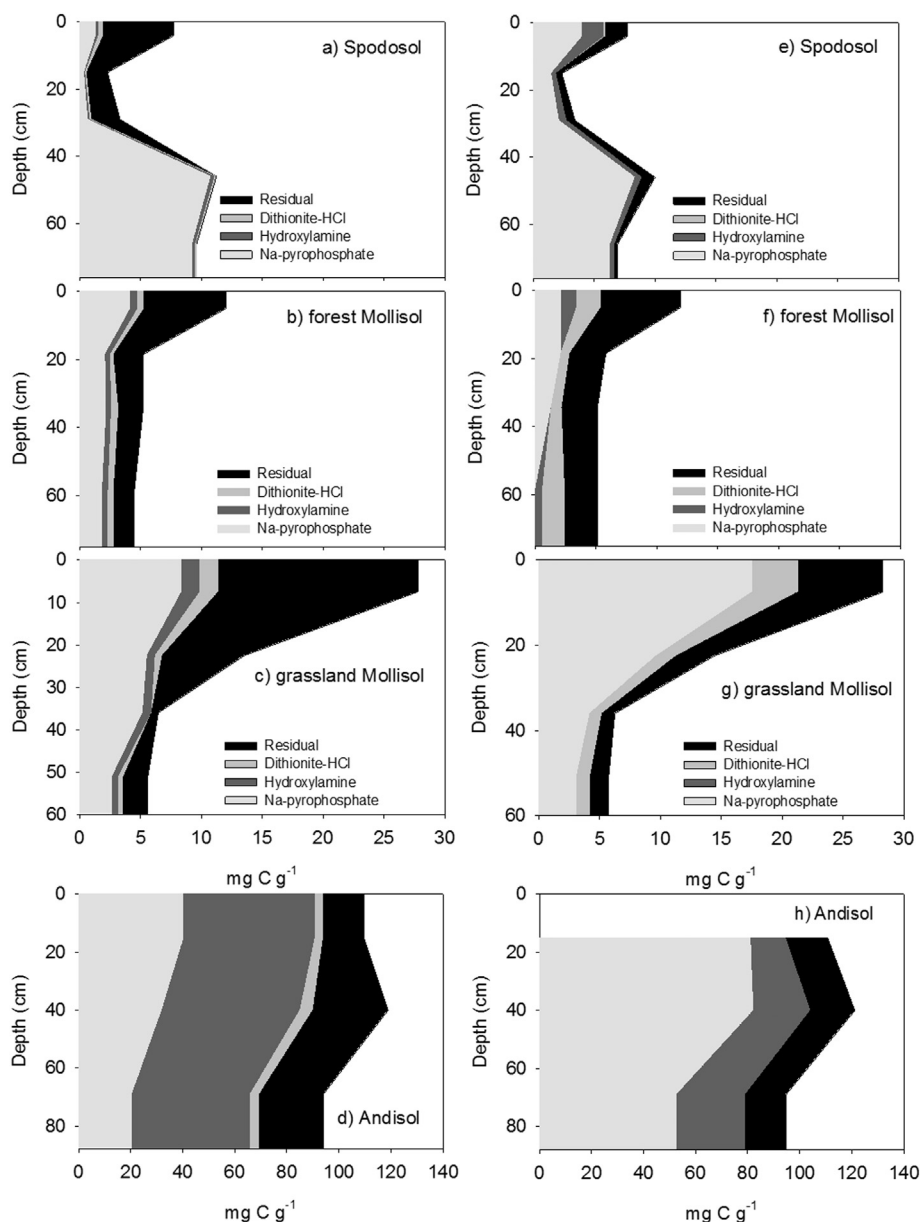


Fig. 2. a–d) Carbon distribution among selective dissolution pools calculated by measurements made on the supernatant solutions. e–h) Carbon distribution among selective dissolution pools calculated by measurements made on the solid fractions after each stage of dissolution.

3.3. Selectively extractable C:Al + Fe molar ratios

We evaluated the ratio of SOC to metals (Al and Fe) extracted using the calculated C content of extracts from the solid-phase method and direct measurements of metal concentrations from the solution-phase measurements (Supp. Table 5). The ratio of the SOC concentration to the combined Al + Fe concentration (M) varied widely with depth and among soils, ranging from 326.7 to 0.1 mol of C mol⁻¹ of Fe + Al (Table 3). In comparison to C, error estimates from replicate measurements of solution-phase Al and Fe concentrations did not increase as dramatically with each subsequent extraction step. Averaged across all soils and depths, standard errors were 7, 10 and 11% of the mean M values for Na-pyrophosphate, hydroxylamine, and dithionite-HCl, respectively. In all soils, C:M decreased in the order Na-pyrophosphate > hydroxylamine > dithionite-HCl. Increasing concentrations of M in all three selective dissolution extracts were positively correlated with the concentration of residual C, bulk soil ¹⁴C abundance and mineral fraction ¹⁴C abundance. Additionally, the concentration of M extracted with Na-pyrophosphate was positively correlated with Na-pyrophosphate extractable C, the solid-phase concentration of C in the

mineral fraction, and the ¹⁴C abundance of the Na-pyrophosphate and dithionite-HCl extractable fractions (Table 4).

4. Discussion

4.1. Application of the sequential selective extraction methodology

New insights into processes contributing to the preservation of SOC have called into question the existence of truly unreactive or “passive” SOC pools, which are assumed to cycle over millennial timescales or longer, and motivated efforts to better characterize the nature of SOC that cycles over decadal to centennial time scales (Schmidt et al., 2011). As such, continued refinement and standardization of methodologies for characterizing SOC pools or classes is essential to conducting temporal comparisons of SOC dynamics within a soil or comparisons between different soils. In particular, a more consistent approach is needed for quantifying the reactivity of slow cycling SOC, which may be susceptible to large scale disturbances such as climate and/or land use change. Here, we have tested an approach for partitioning mineral-associated SOC traditionally thought to comprise this so called passive

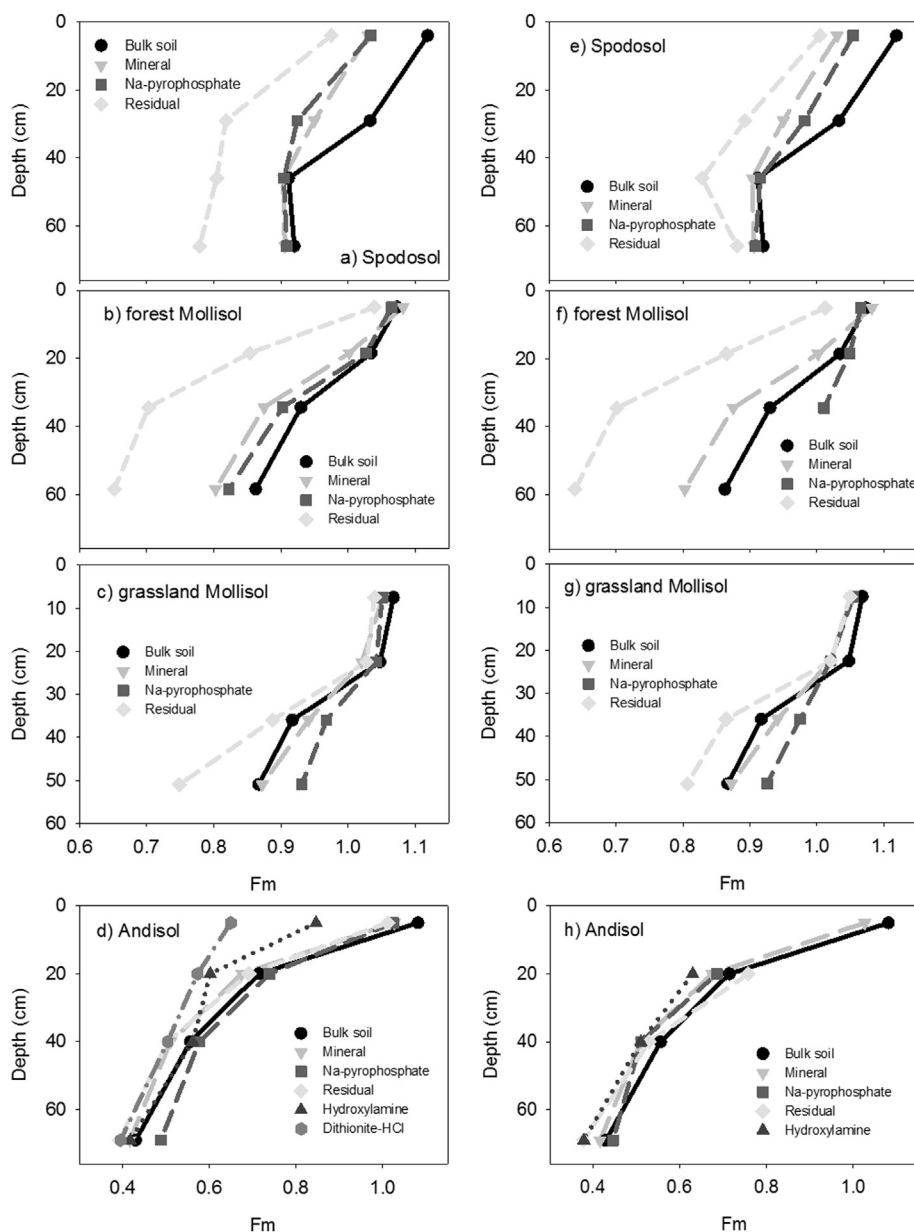


Fig. 3. a–d) Radiocarbon abundance measurements made on the supernatant solutions. e–h) Radiocarbon abundance calculated by measurements made on the solid fractions after each stage of dissolution.

Table 3
Molar ratios of carbon to metal (Al + Fe) in selective dissolution extractions. Values la-beled ND were not-detectable.

Soil	Depth cm	C: Al + Fe (mol: mol)		
		Pyrophosphate	Hydroxylamine	Dithionite HCl
Spodosol	5–8	326.7	41.3	0.7
	22–36	55.8	11.2	ND
	36–56	5.9	1.2	ND
	56–76	5.8	0.9	ND
Forested Mollisol	0–10	3.9	0.4	0.4
	10–27	3.6	ND	0.1
	27–42	2.5	ND	0.1
	42–75	NA	0.2	0.3
Grassland Mollisol	0–15	31.1	ND	1.7
	16–30	25.6	ND	1.2
	31–42	16.9	ND	0.7
	43–60	13.3	ND	0.5
Andisol	10–30	4.2	0.4	ND
	30–50	5.3	0.5	ND
	50–88	3.8	0.6	ND

Table 4
Spearman rank order correlations for Al + Fe concentrations versus C concentrations and radiocarbon (¹⁴C) values for selective dissolution solutions. Negative correlations are reported in parenthesis.

		Pyrophosphate	Hydroxylamine	Dithionite
		Al + Fe mg g ⁻¹ soil		
C mg g ⁻¹ soil	Mineral fraction	0.58*	0.41	0.36
	Pyrophosphate	0.53*	0.24	0.20
	Hydroxylamine	0.44	0.32	0.31
	Dithionite	(0.41)	0.03	< 0.01
	Residual	0.57*	0.83***	0.78***
¹⁴ C (Fm)	Bulk soil	0.65*	0.56*	0.63*
	Mineral fraction	0.59*	0.58*	0.64*
	Pyrophosphate	0.61*	0.39	0.46
	Hydroxylamine	(0.10)	0.17	0.16
	Dithionite	0.57*	0.15	0.18

* indicates p < 0.05.
*** indicates p < 0.001.

pool. Specifically, we examined the distribution and ^{14}C signature of SOC associated with distinct mineral associations in four soils of widely differing morphology. Within each of these soil types, we also considered depth gradients of SOC operationally partitioned by density separation and sequential selective dissolution.

A primary goal of this work was to test the hypothesis that sequential chemical dissolution techniques allow for quantification of soil mineral functional classes and measurements of the SOC associated with them. Specifically, we examined the utility of a three-step sequential selective extraction procedure, combining individual methods often used in isolation or in parallel extractions to estimate the abundance of minerals of varying crystallinity (Wagai et al., 2013). This approach is novel in that we have either measured directly or calculated the C concentrations and radiocarbon content liberated during each step. This method allows for improved characterization of the stocks and turnover times of mineral-associated SOC or the “passive” pool. Our results, showing SOC with distinct radiocarbon content is isolated through each stage of the procedure, supports the hypothesis that sequential selective chemical dissolution can be used to partition SOC protected through interactions with different minerals. These methods, however, are not without significant challenges. Below, we discuss some limitations of the method, lessons learned for future application, and general insights from results of this study.

Preliminary testing indicated that separation of the soil mineral fraction, in this case using density, was a necessary precursor for successful application of the sequential mineral dissolution procedure. It must be noted, however, that density separation is subject to an additional set of assumptions and errors. In particular, the density threshold needed to maximize the distinction between C pools (based on ^{14}C content) may vary by soil type (Crow et al., 2007). For the purpose of this study, we assumed that the use of a similar threshold of 1.65 resulted in consistent partitioning of light and heavy pools across all soils evaluated. Additionally, density separation may result in mobilization of, in some cases, up to 25% of the total C in the SPT solution (e.g., Crow et al., 2007). We attribute low C recoveries from some samples to mobilization in SPT; however, we did not measure these losses of C directly. For future application of these density separation procedures, we strongly recommend measuring the C content of the SPT solution. Despite these limitations, performing the density separation prior to the sequential selective extraction of the mineral fraction limits contributions from organics that could become solubilized from particulate organic matter (free-light and occluded fractions). Density fractionation also demonstrated the importance of mineral association for SOC dynamics. Across all the soils studied, a large fraction (0.25 to 0.99) of the total bulk C pool was attributable to the mineral-associated fraction. Soil OC associated with mineral fractions was consistently depleted in ^{14}C (i.e., older C) compared with the free-light fractions and with the occluded fractions in three out of the four soils examined (Fig. 1; forested Mollisol occluded fraction contained a substantial amount of pyrogenic material). While this finding is not novel (Swanston et al., 2005), together these observations highlight the role of minerals as a control on the transit time of C through soils. Variations between soils in the ^{14}C content of the mineral-associated fraction likely reflect differences in the stability of the organo-mineral bonds or climatic influences. In this study, we have presented one method—a sequential selective chemical extraction—for improved characterization of variability in the abundance and stability of different mineral associations contributing to mass of SOC isolated through density separation of the mineral fraction.

Starting with the mineral fraction isolated from the density separation, we measured both the amounts of C extracted in the aqueous phases and the corresponding change in the concentration of the residual solid phase following each extraction step. Generally, these two approaches yielded similar results, suggesting that the methods are internally consistent (Fig. 4). Owing to the complications in making measurements on the selective dissolution supernatant solutions,

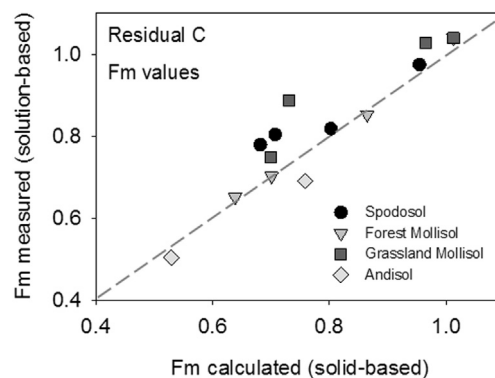


Fig. 4. Comparison of Fraction Modern (Fm) radiocarbon values as measured by the solution-based and solid-based approaches. Close 1: 1 correlation between the two approaches supports the reliability of the solid-based approach. Only Na-pyrophosphate extractable and residual values are used due to the paucity of data on hydroxylamine and dithionite-HCl extracts.

however, we recommend using the solid-based approach in future investigations. Additionally, we advise extracting > 1 g of soil for most locations as we were not able to extract enough SOC from the sequential hydroxylamine and dithionite-HCl extractions, except from the Andisol samples, to adequately characterize radiocarbon content. For most soils, extraction at least 5 g of soil would likely yield better results. When scaling up this method, it is important to consider the sample to solution ratio. In this study, we used a ratio of 1 g sample (starting with the mineral fraction density separate) to 40 ml extractant. With a 5 g sample size, this would require 200 ml of extractant to yield the same ratio and thus would require using larger centrifuge tubes. In soils with very low SOC content, it may be preferable to use a parallel extraction approach rather than a sequential one. Parallel extractions, however, require calculating the abundance of C and metals from individual mineral pools by the difference between individual extraction results (e.g., Masiello et al., 2004), which can create mass balance issues on account of the non-unique nature of these extractions.

4.2. Further partitioning the mineral fraction

The first extraction in the sequence targets organo-metal complexes which represent a significant portion of the mineral associated C. Na-pyrophosphate extractable C was first examined by Bascomb (1968) and Goh et al. (1976) where it was identified as a potential morphological characterization tool, but since then has been used to show a strong correlation of Al and Fe extracted with the total and bulk SOC (Masiello et al., 2004; Wagai et al., 2013; Lawrence et al., 2015; Takahashi and Dahlgren, 2016). It is generally assumed that Al and Fe extracted with Na-pyrophosphate are derived from amorphous organo-metal complexes. We cautiously apply this interpretation, as there is evidence Na-pyrophosphate may also dissolve additional Al-bearing minerals (Kaiser and Zech, 1996). In all four of the soil profiles examined here, Na-pyrophosphate extractions removed a large fraction of the total C pool, averaging 0.3 to 0.43 (depending on the method used), of the total SOC attributable to the mineral separates. This result is consistent with the value of 0.3 reported in Wagai et al. (2013).

The radiocarbon content of Na-pyrophosphate extractable C, which was similar to bulk values but more ^{14}C enriched compared with the mineral fraction, suggests an intermediate residence time for this pool of C in the soil. Carbon concentration and radiocarbon abundance of the Na-pyrophosphate extractable C pool were positively correlated with the concentration of Na-pyrophosphate extractable metals (Fig. 4) suggesting isolation of a unique C reservoir, likely associated with organo-metal complexes and/or amorphous metal hydroxide phases. However, the actual mechanistic underpinnings of Na-pyrophosphate extraction remain undefined and the method currently cannot

distinguish between C extracted through peptization and base solubility (Kaiser and Zech, 1996; Pansu and Gautheyrou, 2006). For example, in a comparison of base-soluble and Na-pyrophosphate soluble organic matter (OM) pools, Wagai et al. (2013) found that base solubility accounted for approximately 80% of the Na-pyrophosphate extractable pool. Further examination of the composition of Na-pyrophosphate extractable C is necessary in order to confirm that it is a functionally distinct pool of soil C, but our results provide additional support for the idea that organo-metal complexes are at least an important intermediary step in the long-term preservation of SOC (Lawrence et al., 2015).

Hydroxylamine-extractable C, thought to be associated with SRO Fe- and Al-hydroxide phases (e.g. ferrihydrite, allophane, imogolite), accounted for a small but measureable portion of total mineral-stabilized C in the three temperate soils examined. Our findings are once again consistent with those of Wagai et al. (2013) who also found that Na-pyrophosphate extractable OM accounted for the majority of selectively dissolvable OM in soils. As expected, the hydroxylamine extractable pool was greatest in the allophanic Hawaiian Andisol, which is known to have a high concentration of SRO minerals (Torn et al., 1997; Cornell and Schwertmann, 2003; Kramer and Chadwick, 2016). Unfortunately, graphitization of hydroxylamine extractions proved difficult. The few radiocarbon values that we measured suggest that hydroxylamine-extractable C may be more stable (as inferred from relative depletion of ^{14}C abundance) than the unextractable residual pool in some soils (Supp. Table 3). While too few values were obtained to make strong inferences, the hydroxylamine-extractable radiocarbon values measured on the grassland Mollisol were depleted in comparison to the residual C values, possibly providing additional evidence that selective dissolutions isolate uniquely cycling pools of C associated with specific mineral phases, rather than (or in addition to) solely dissolving acid/base soluble C. From previous studies, which did not directly measure the radiocarbon content of C associated with SRO minerals, there is a general consensus, based on correlations of bulk SOC radiocarbon with SRO content, that SRO associations provide long-term stabilization of SOC.

Our results indicate that SRO- (hydroxylamine-) associated C is not the most ^{14}C -depleted (i.e., stable) pool of C present in the Andisol soils tested here (Fig. 3d, h). This runs counter to the common inference that SRO phases such as allophane, imogolite and ferrihydrite are responsible for the stabilization of the large SOM pools found in these soils (Harsh et al., 2002; Liliencron et al., 2004). Taken as a whole, these data may suggest that the abundance of SRO minerals is a correlative proxy for the total C sorption and retention capacity of the soil, but is not an indication that SRO phases are the most important or effective surfaces for C sorption in these soils.

We interpret the dithionite-HCl extraction step as targeting primarily secondary crystalline mineral phases and any C associated with those phases. This reservoir of C was very small or undetectable in the three temperate soils examined, despite the high concentrations of metals, primarily Fe, that were extracted with dithionite-HCl (Supp. Table 5). These results suggest the majority of mineral-associated C was removed in the earlier extraction steps and that the more crystalline minerals, which are extracted during the dithionite-HCl step, may not be directly responsible for stabilization of much SOC. Although dithionite-HCl extractable C is sometimes correlated with bulk SOC (e.g., Heckman et al., 2009), the small amounts of C we observed are consistent with abundance of crystalline Fe fractions that were isolated through a sequential density fractionation procedure (Sollins et al., 2006, 2009). Owing to the small amounts of C in the dithionite-HCl extractions, we were unable to make reliable measurements of the radiocarbon for any soils except the Andisol. However, the few measures of dithionite-HCl extracted C were more ^{14}C depleted than any other reservoir measured from the Andisol soils. This suggests that while there is little C associated with the crystalline phases, what is there is very stable. The sequential density separation approach

mentioned previously (Sollins et al., 2006, 2009) has indicated crystalline fractions, dominated by quartz and feldspars and assumed to possess unreactive surfaces, to be more ^{14}C depleted than fractions dominated by secondary phyllosilicates. This observation supports the idea that sorption to Fe-poor crystalline surfaces could play an important role in regulating small but highly stable fractions of SOC. Future work with this method should utilize a larger starting sample mass if enough C is to be extracted to confirm this observation for other soils.

For the majority of the soils we measured, residual SOC remaining after all extraction steps accounted for a sizeable fraction (average of 31%) of the total C in the mineral separates (Fig. 1). Furthermore, residual C from the three temperate soils was ^{14}C depleted in comparison to all other sequentially isolated mineral reservoirs. In contrast, the residual C from the Andisol was similarly or less ^{14}C depleted (younger) than either the dithionite-HCl or hydroxylamine extractable C. We might assume that base-soluble C will always be younger in comparison to the insoluble fraction, and that this result may be merely the product of base-solubility chemistry rather than reflective of differences in the stability of organo-metal and organo-mineral associations. However, radiocarbon measurements of SOC fractions separated using the classical fulvic/humic/humin method suggests that the acid/base insoluble fraction of SOC is not always the most ^{14}C depleted (Martel and LaSalle, 1977; Anderson and Paul, 1984). Although the form and mechanism of stabilization of the residual C isolated in this study is not entirely clear, the significant abundance and high degree of ^{14}C depletion in all of the soils studied suggest such residual C could be an important reservoir of highly stable or “passive” SOC. Future work on this topic should seek to characterize the form of C in the residual phase with the goal of evaluating whether it is a natural reservoir common to soils or an artefact of a highly aggressive fractionation procedure.

5. Summary

We utilized a multistep, density and sequential chemical extraction procedure, which leveraged existing methodologies, for fractionating soils in a novel fashion. This procedure allowed for quantification of metals (i.e., Fe and Al) resulting from the dissolution of distinct mineral phases and SOC associated with those minerals. The result of this testing supported our first hypothesis, that the sequential chemical extraction allows for isolation of distinct SOC fractions, as differentiated by unique radiocarbon content, and provides a tool for better characterization of passive C in soils.

The procedure described here, however, is not without challenges. The sequential nature of the method dictates that sufficient sample mass is used in order to extract enough SOC from each step for adequate measurements. Furthermore, graphitization of extracts proved challenging and additional refinement of the method is required in order to improve the reliability and repeatability of radiocarbon measurements. One promising approach that we tested involved measuring changes in the residual solid phase after each extraction step. Our results indicated that this is a viable option but, again, sufficient starting sample mass must be used. Overall, this methodology is time consuming and if problems arise during any stage of the process, the dissolution procedure must be repeated from the beginning. Despite such challenges, this method offers great potential for improved characterization of slow-cycling SOC reservoirs in a way that may be paired with mineral-enabled models of C cycling (e.g., Lawrence et al., 2014; Riley et al., 2014).

In support of our second hypothesis, we observed clear differences in the four soils we tested, which were consistent with our expectations. In particular, the Andic soils contained significantly greater amounts of short-range order minerals, and SOC associated with those minerals, compared with all other soils. Additionally, the Spodic soil exhibited depletion of metal and SOC in the E horizon and characteristic enrichment of organo-metal complexes in the Bhs horizons. Taken

together, such observations suggest this method adequately targets different mineral groups and the C associated with those minerals.

Radiocarbon measurements of C fractions isolated through the sequential selective extraction procedure differed between each extractant and the soils tested, supporting our third hypothesis. For example, in most soils at most depths, SOC extracted with Naprophosphate was generally ^{14}C depleted in comparison to the mineral fraction as a whole, suggesting a younger age and possibly shorter residence time of organo-metal complexed C relative to other mechanisms of mineral stabilization. In contrast, all soils exhibited a portion of extraction-resistant, or residual, C characterized by a high degree of ^{14}C depletion (i.e., older C), which may be indicative of a millennial scale (passive) C pool. Furthermore, depth dependent differences in sequentially extracted C pools, such as greater ^{14}C depletion of hydroxylamine extractable C compared with other C liberated from shallow depths of the Andisol, may be diagnostic of the relationship between soil development and the preservation of SOC.

Overall, our results suggest the potential of the sequential selective extraction technique as a tool to better characterize the nature of C-mineral associations in soils. Such an approach is necessary in order to understand the dynamic nature of soil C pools that have been erroneously considered as unreactive in our conceptual models. More work is required to refine this technique so that it may be broadly applied and so that we can increase confidence in our interpretations of the various pools of minerals and C that are extracted. For example, molecular characterization of the C associated with the various selective dissolution extractions would offer additional and powerful insight into the nature and effectiveness of isolating C associated with different mineral classes. Additionally, characterization of changes in the properties of the residual solid-phase, such as reactive surface area measurements, after each extraction step may provide added insight into the nature of mineral-C bonding. Combined with C abundance and radiocarbon content, these additional measurements will provide the necessary information for more detailed inclusion of C-mineral associations in a new generation of C-enabled reactive transport models (Li et al., 2017).

Supplementary data to this article can be found online at <https://doi.org/10.1016/j.geoderma.2017.09.043>.

Acknowledgments

We thank Dr. Courtney Creamer for thoughtful comments on an early version of this manuscript. This work was supported by the U.S. Geological Survey Climate and Land Use Mission Area. Radiocarbon analysis was sponsored by the Radiocarbon Collaborative, which is jointly supported by the U.S. Department of Agriculture Forest Service, University of California Irvine, and Michigan Technological University. Any use of trade, firm, or product names is for descriptive purposes only and does not imply endorsement by the U.S. Government.

References

- Anderson, D.W., Paul, E.A., 1984. Organo-mineral complexes and their study by radiocarbon dating. *Soil Sci. Soc. Am. J.* 48 (2), 298–301.
- Bascomb, C.L., 1968. Distribution of pyrophosphate-extractable iron and organic carbon in soils of various groups. *J. Soil Sci.* 19 (2), 251–268.
- Cornell, R.M., Schwertmann, U., 2003. *The Iron Oxides: Structure, Properties, Reactions, Occurrences and Uses*. John Wiley & Sons, Heppenheim, Germany.
- Crow, S.E., Swanston, C.W., Lajtha, K., Brooks, J.R., Keirstead, H., 2007. Density fractionation of forest soils: Methodological questions and interpretation of incubation results and turnover time in an ecosystem context. *Biogeochemistry* 85, 69–90.
- Dahlgren, R.A., 1994. Quantification of allophane and imogolite. In: Amonette, J.E., Zelazny, L.W. (Eds.), *Quantitative Methods in Soil Mineralogy*. SSSA Inc., Madison, WI, pp. 430–451.
- Essington, M.E., 2004. *Soil and water chemistry: An integrative approach*. CRC Press, Boca Raton, FL, pp. 311–397.
- Eusterheus, K., Rumpel, C., Kogel-Knabner, I., 2005. Organo-mineral associations in sandy acid forest soils: importance of specific surface area, iron oxides and micropores. *Eur. J. Soil Sci.* 56, 753–763.
- Goh, K.M., Rafter, T.A., Stout, J.D., Walker, T.W., 1976. The accumulation of soil organic matter and its carbon isotope content in a chronosequence of soils developed on

- aeolian sand in New Zealand. *J. Soil Sci.* 27, 89–100.
- Hall, S.J., Silver, W.L., 2013. Iron oxidation stimulates organic matter decomposition in humid tropical forest soils. *Glob. Chang. Biol.* 19, 2804–2813.
- Han, Z., Franssen, H.-J.H., Montzka, C., Vereecken, H., 2014. Soil moisture and soil properties estimation in the Community Land Model with synthetic brightness temperature observations. *Water Resour. Res.* 50 (7), 6081–6105.
- Harsh, J., Chorover, J., Nizeyimana, E., 2002. Allophane and imogolite. In: Dixon, J.B., Schulze, D.G. (Eds.), *Soil Mineralogy with Environmental Applications*. Soil Science Society of America Inc, Madison, Wisconsin, pp. 291–322.
- Heckman, K., Welty-Bernard, A., Rasmussen, C., Schwartz, E., 2009. Geologic controls of soil carbon cycling and microbial dynamics in temperate conifer forests. *Chem. Geol.* 267 (1), 12–23.
- Heckman, K., Vazquez-Ortega, A., Gao, X., Chorover, J., Rasmussen, C., 2011. Changes in water extractable organic matter during incubation of forest floor material in the presence of quartz, goethite and gibbsite surfaces. *Geochim. Cosmochim. Acta* 75, 4295–4309.
- Heckman, K., Throckmorton, H., Clingensmith, C., González Vila, F.J., Horwath, W.R., Knicker, H., Rasmussen, C., 2014. Factors affecting the molecular structure and mean residence time of occluded organics in a lithosequence of soils under ponderosa pine. *Soil Biol. Biochem.* 77, 1–11.
- Kahle, M., Kleber, M., Jahn, R., 2002. Carbon storage in loess derived surface soils from Central Germany: Influence of mineral phase variables. *J. Plant Nutr. Soil Sci.* 165, 141–149.
- Kahle, M., Kleber, M., Jahn, R., 2003. Retention of dissolved organic matter by illitic soils and clay fractions: influence of mineral phase properties. *J. Plant Nutr. Soil Sci.* 166, 737–741.
- Kaiser, K., Zech, W., 1996. Defects in estimation of aluminum in humus complexes of podzolic soils by pyrophosphate extraction. *Soil Sci.* 161 (7), 452–458.
- Keiluweit, M., Keber, M., 2009. Molecular-level Interactions in soils and sediments: The role of aromatic π -systems. *Environ. Sci. Technol.* 43, 3421–3429.
- Kögel-Knabner, I., Guggenberger, G., Kleber, M., Kandeler, E., Kalbitz, K., Stefan, S., Eusterheus, K., Leinweber, P., 2008. Organo-mineral associations in temperate soils: Integrating biology, mineralogy, and organic matter chemistry. *J. Plant Nutr. Soil Sci.* 171, 61–82.
- Kramer, M.G., Chadwick, O.A., 2016. Controls on carbon storage and weathering in volcanic soils across a high-elevation climate gradient on Mauna Kea, Hawaii. *Ecology* 97 (9), 2384–2395. <http://dx.doi.org/10.1002/ecy.1467>.
- Recarbonization of the biosphere: ecosystems and the global carbon cycle. In: Lal, R., Lorenz, K., Hüttl, R.F., Schneider, B.U., von Braun, J. (Eds.), *Springer Science & Business Media*.
- Lawrence, C., Harden, J.W., Maher, K., 2014. Modeling the influence of organic acids on soil weathering. *Geochim. Cosmochim. Acta* 139, 487–507.
- Lawrence, C., Harden, J.W., Xu, X., Schulz, M.S., Trumbore, S.E., 2015. Long-term controls on soil organic carbon with depth and time: a case study from the Cowlitz River chronosequence, WA USA. *Geoderma* 247–248, 73–87.
- Li, L., Maher, K., Navarre-Stichler, A., Druhan, J., Meile, C., Lawrence, C., et al., 2017. Expanding the role of reactive transport models in critical zone processes. *Earth Sci. Rev.* 165 (C), 280–301. <http://dx.doi.org/10.1016/j.earscirev.2016.09.001>.
- Lilienfein, J., Qualls, R.G., Uselman, S.M., Bridgman, S.D., 2004. Adsorption of dissolved organic carbon and nitrogen in soils of a weathering chronosequence. *Soil Sci. Soc. Am. J.* 68, 292–305.
- Litton, C.M., Giardina, C.P., Albano, J.K., Long, M.S., Asner, G.P., 2011. The magnitude and variability of soil-surface CO₂ efflux increase with mean annual temperature in Hawaiian tropical montane wet forests. *Soil Biol. Biochem.* 43, 2315–2323.
- von Lütow, M.V., Kögel-Knabner, I., Ekschmitt, K., Matzner, E., Guggenberger, G., 2006. Stabilization of organic matter in temperate soils: mechanisms and their relevance under different soil conditions: a review. *Eur. J. Soil Sci.* 57, 426–445.
- Martel, Y.A., LaSalle, P., 1977. Radiocarbon dating of organic matter from a cultivated topsoil in eastern Canada. *Can. J. Soil Sci.* 57 (3), 375–377.
- Masiello, C.A., Chadwick, O.A., Southon, J., Torn, M.S., Harden, J.W., 2004. Weathering controls on mechanisms of carbon storage in grassland soils. *Glob. Biogeochem. Cycles* 18 doi:10.1029/2004GB002219.
- Mikutta, R., Kleber, M., Torn, M.S., Jahn, R., 2006. Stabilization of soil organic matter: association with minerals or chemical recalcitrance? *Biogeochemistry* 77, 25–56.
- Oades, J.M., 1988. The retention of organic-matter in soils. *Biogeochemistry* 5 (1), 35–70.
- Pansu, M., Gautheyrou, J., 2006. *Mineralogical separation by selective dissolution*. In: *Handbook of Soil Analysis: Mineralogical, Organic and Inorganic Methods*. Springer Science & Business Media, pp. 167–219.
- Parfitt, R.L., 2009. Allophane and imogolite: role in soil biogeochemical processes. *Clay Miner.* 44, 135–155.
- Parfitt, R.L., Childs, C.W., 1988. Estimation of forms of Fe and Al: a review, and analysis of contrasting soils by dissolution and Moessbauer methods. *Aust. J. Soil Res.* 26, 121–144.
- Percival, H.J., Parfitt, R.F., Scott, N.A., 1999. Factors controlling soil carbon levels in New Zealand grasslands: Is clay content important? *Soil Sci. Soc. Am. J.* 65, 1623–1630.
- Rasmussen, C., Torn, M.S., Southard, R.J., 2005. Mineral assemblage and aggregates control carbon dynamics in a California conifer forest. *Soil Sci. Soc. Am. J.* 69, 1711–1721.
- Rasmussen, C., Southard, R.J., Horwath, W.R., 2006. Mineral control of organic carbon mineralization in a range of temperate conifer forest soils. *Glob. Chang. Biol.* 12, 834–847.
- Riley, W.J., Maggi, F., Kleber, M., Torn, M.S., Tang, J.Y., Dwivedi, D., Guerry, N., 2014. Long residence times of rapidly decomposable soil organic matter: application of a multi-phase, multi-component, and vertically resolved model (BAMS1) to soil carbon dynamics. *Geosci. Model Dev.* 7 (4), 1335–1355. <http://dx.doi.org/10.5194/gmd-7-1335-2014>.

- Ross, G.J., Wang, C., Schuppli, P.A., 1985. Hydroxylamine and ammonium oxalate solutions as extractants for iron and aluminum from soils. *Soil Sci. Soc. Am. J.* 49, 783–785.
- Saidy, A.R., Smernik, R.J., Baldock, J.A., Kaiser, K., Sanderman, J., Macdonald, L.M., 2012. Effects of clay mineralogy and hydrous iron oxides on labile organic carbon stabilization. *Geoderma* 173, 104–110.
- Schaetzl, R.J., 2002. A Spodosol-Entisol transition in northern Michigan. *Soil Sci. Soc. Am. J.* 66 (4), 1272–1284.
- Schmidt, M.W., Torn, M.S., Abiven, S., Dittmar, T., Guggenberger, G., Janssens, I.A., Kleber, M., Kögel-Knabner, I., Lehmann, J., Manning, D.A., Nannipieri, P., 2011. Persistence of soil organic matter as an ecosystem property. *Nature* 478 (7367), 49–56.
- Schulz, M.S., Vivit, D., Schulz, C., Fitzpatrick, J., White, A., 2010. Biologic origin of iron nodules in a marine terrace chronosequence, Santa Cruz, California. *Soil Sci. Soc. Am. J.* 74 (2), 550–564.
- Sollins, P., Swanston, C., Kleber, M., Filley, T., Kramer, M., Crow, S., Caldwell, B.A., Lajtha, K., Bowden, R., 2006. Organic C and N stabilization in a forest soil: evidence from sequential density fractionation. *Soil Biol. Biochem.* 38 (11), 3313–3324.
- Sollins, P., Kramer, M.G., Swanston, C., Lajtha, K., Filley, T., Aufdenkampe, A.K., Wagai, R., Bowden, R.D., 2009. Sequential density fractionation across soils of contrasting mineralogy: evidence for both microbial- and mineral-controlled soil organic matter stabilization. *Biogeochemistry* 96, 209–231.
- Strickland, T.C., Sollins, P., 1987. Improved method for separating light-fraction and heavy-fraction organic material from soil. *Soil Sci. Soc. Am. J.* 51, 1390–1393.
- Stuiver, M., Polach, H.A., 1977. Discussion: reporting of ¹⁴C data. *Radiocarbon* 19, 355–363.
- Swanston, C., Torn, M., Hanson, P., Southon, J., Garten, C., Hanlon, E.M., Ganio, L., 2005. Initial characterization of processes of soil carbon stabilization using forest stand-level radiocarbon enrichment. *Geoderma* 128, 52–62.
- Tadros, T., 2013. Chapter 195: Ostwald ripening. In: *Encyclopedia of Colloid and Interface Science*. Springer Berlin Heidelberg, pp. 820.
- Takahashi, T., Dahlgren, R.A., 2016. Nature, properties and function of aluminum–humus complexes in volcanic soils. *Geoderma* 263, 110–121.
- Tiessen, H., Stewart, J.W.B., Hunt, H.W., 1984. Concepts of soil organic matter transformations in relation to organo-mineral particle size fractions. *Plant Soil* 76, 287–295.
- Torn, M.S., Trumbore, S.E., Chadwick, O.A., Vitousek, P.M., Hendricks, D.M., 1997. Mineral control of soil organic carbon storage and turnover. *Nature* 389, 170–173.
- Trumbore, S., 2009. Radiocarbon and soil carbon dynamics. *Ann. Rev. Earth Pl. Sci.* 37, 47–66.
- Vogel, J.S., Southon, J.R., Nelson, D.E., 1987. Catalyst and binder effects in the use of filamentous graphite for AMS. *Nucl. Instrum. Method B* 29, 50–56.
- Wagai, R., Mayer, L.M., 2007. Sorptive stabilization of organic matter in soils by hydrous iron oxides. *Geochim. Cosmochim. Acta* 71, 25–35.
- Wagai, R., Mayer, L.M., Kiyama, K., Shirato, Y., 2013. Association of organic matter with iron and aluminum across a range of soils determined via selective dissolution techniques coupled with dissolved nitrogen analysis. *Biogeochemistry* 112, 95–109.
- White, A.F., Schulz, M.S., Vivit, D.V., Blum, A.E., Stonestrom, D.A., Anderson, S.P., 2008. Chemical weathering of a marine terrace chronosequence, Santa Cruz, California I: interpreting rates and controls based on soil concentration–depth profiles. *Geochim. Cosmochim. Acta* 72 (1), 36–68.
- White, A.F., Schulz, M.S., Stonestrom, D.A., Vivit, D.V., Fitzpatrick, J., Bullen, T.D., Maher, K., Blum, A.E., 2009. Chemical weathering of a marine terrace chronosequence, Santa Cruz, California. Part II: solute profiles, gradients and the comparisons of contemporary and long-term weathering rates. *Geochim. Cosmochim. Acta* 73 (10), 2769–2803.